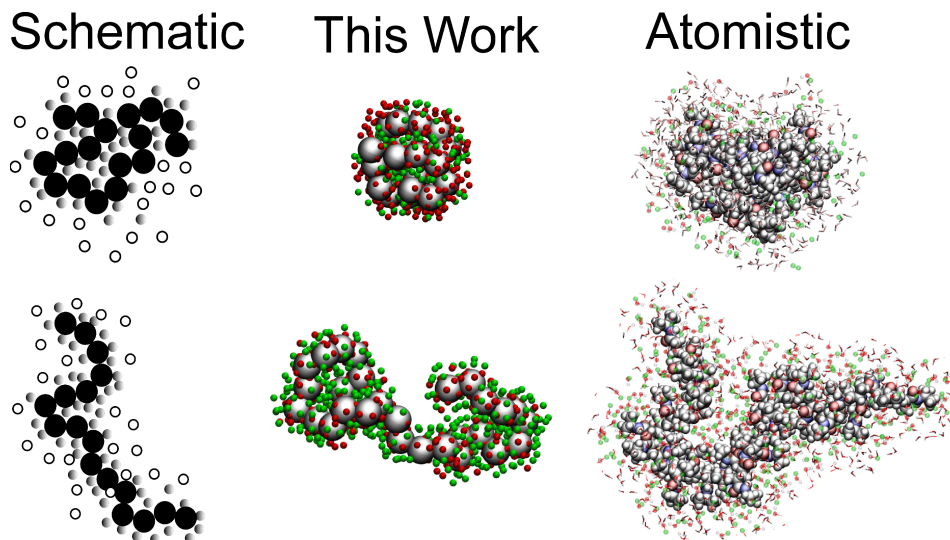
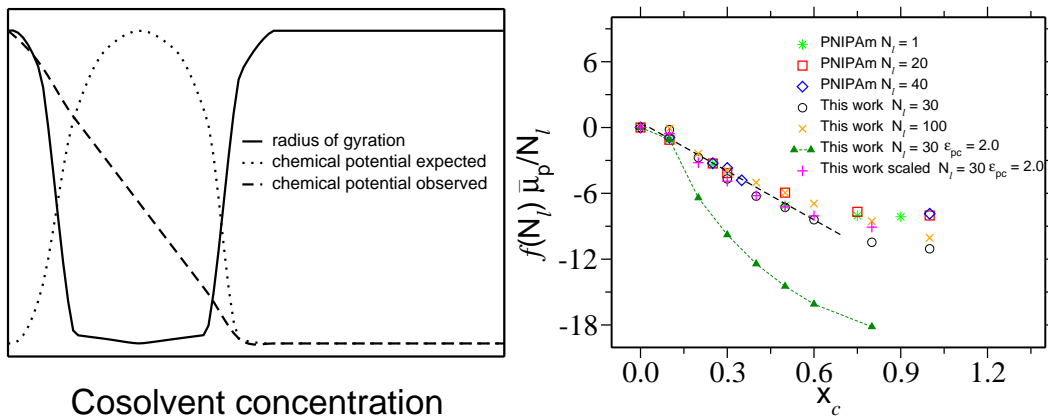


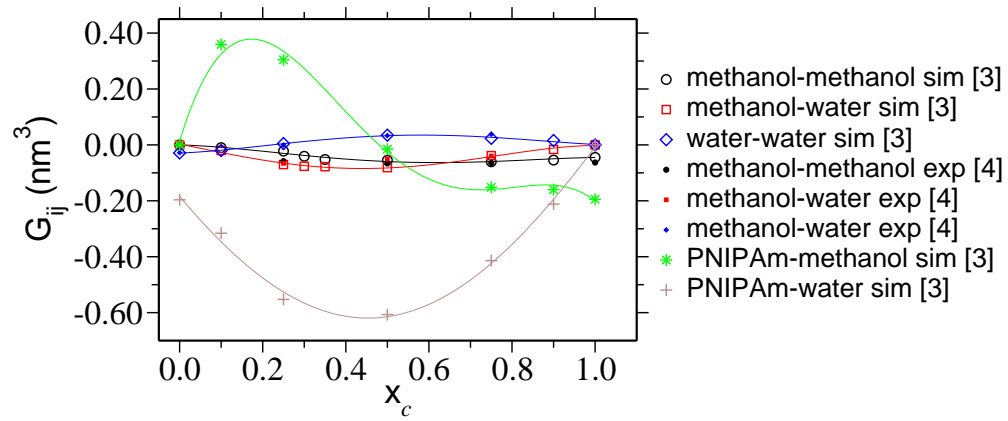
Supplementary Figure 1: Conformation of polymer. Radius of gyration R_g as a function of chain length N_l for three different methanol mole fractions x_c .



Supplementary Figure 2: Simulation snapshots showing the collapsed globule and extended coil conformations of a polymer. The atomistic configurations are taken from Ref. [3] and the bead-spring configurations are the snapshots from this work. For the more prominent illustration of molecular binding, we also draw a schematic picture. In atomistic representation: hydrogen of methanol is shown in silver, oxygen of methanol is shown in red, united atom CH_3 is shown in green. The water molecules are drawn as transparent line representation. For bead-spring representation: red spheres mimic water and green is used to mimic methanol. In schematic representation: empty circles mimic water and grey circles mimic methanol. The simulations snapshots for collapsed globule are taken for $x_c = 0.10$ for both atomistic and bead-spring. For coil state, we take a configuration at $x_c = 0.35$ for atomistic and $x_c = 0.60$ for bead-spring. Note that there is typographical error in the caption to Fig. 5 of Ref. [3], the extended configuration corresponds to $x_c = 0.35$, which was wrongly stated as $x_c = 0.75$.



Supplementary Figure 3: Thermodynamics of polymer collapse. (Left panel) Schematic representation of radius of gyration R_g and chemical potential μ_p of polymer in mixed solvents. We show μ_p plot, which is to be expected from the behavior of R_g as a function of cosolvent concentration and the originally observed μ_p [3]. (Right panel) Chemical potential shift $\bar{\mu}_p$ per monomer as a function of cosolvent mole fraction x_c . $\bar{\mu}_p$ obtained from the generic model is compared to the data from the atomistic configuration of PNIPAm, which is taken from Ref. [3]. The master curve is obtained by normalizing the $\bar{\mu}_p$ with a chain length N_l dependent function $f(N_l) = 2N_l/(N_l + 1)$. The scaled data corresponding to $\epsilon_{pc} = 2.0\epsilon$ is normalized by a factor of 2. The lines are drawn to guide the eye.



Supplementary Figure 4: Excess coordination. Kirkwood-Buff integral G_{ij} between different solution components as a function of cosolvent molar fraction x_c . The data was obtained from the semi-grand canonical simulations incorporating all-atom details [3]. For the comparison, we have also included experimental data taken from Ref. [4].

Supplementary Note 1: The Flory Exponent

In the main text we have discussed the effect of chain length N_l on the coil-globule-coil transition. Here we want to look into the scaling of the radius of gyration R_g . The conformation of polymers can be characterized by the scaling exponents, which suggests $R_g \approx N_l^\nu$. In the mean-field theory, the exponent $\nu = 3/(2 + d)$ for good solvent and $\nu = 1/d$ for poor solvent in d -dimension [1]. In Fig. 1 we show N_l dependent R_g . The exact value of ν was found to be 0.588 ± 0.001 , in three dimension, using renormalization group theory [2]. In our simulations, we find $\nu = 0.61$ at $x_c = 0$ (good solvent), $\nu = 0.34$ at $x_c = 0.1$ (poor solvent) and $\nu = 0.58$ at $x_c = 0.8$ (good solvent). Further suggesting that the polymer has gone through a coil-globule-coil transition. Note that we only choose three different N_l . The data corresponding to $N_l = 10$ was only used to estimate ν . Considering the short N_l and also ν values are estimated from three data points, the observed values of ν are in good agreement with the mean field prediction.

Supplementary Note 2: All-atom vs Generic Simulations

In the main text we have shown that the generic model reproduces correct intermolecular binding. Here, we show simulation snapshots to make an one-to-one correspondence with the all-atom data. In Fig. 2, we compare atomistic simulation snapshots with the generic model. For better illustration intermolecular binding scenario, we have also included schematic representations of both globule and coil states. Since the conformational transition is strongly driven by the cosolvent interactions, we tune the solute-cosolvent interactions in the generic model to mimic preferential binding. It can be seen from the schematic representation of globule that the cosolvent molecules usually arrange themselves within the interstitial positions, making a bridge between two distant monomer contact. This is exactly observed in our generic simulations, where the green spheres, mimicking cosolvents, are situated in the interstitial positions when the polymer collapses into a globule. Moreover, when the cosolvent concentration is increased, more cosolvent molecules shields the polymer to form an extended coil structure of the polymer. More interestingly, both observations are found to be in strikingly good agreement with the atomistic configurations obtained from the multiscale simulations [3].

Supplementary Note 3: Chemical Potential and The Effect of Polymer Cosolvent Interaction

In the main text we have shown that the chemical potential shift $\bar{\mu}_p$ per monomer systematically decreases even when the polymer remains in a collapse state. Moreover, within a mean field description, if a polymer goes through coil-globule-coil transition, then $\bar{\mu}_p$ should also increased where polymer collapses, as shown in the schematic Fig. 3. This makes the Flory-Huggins type mean field picture unsuitable and therefore a discrete particle based approach is needed to understand these complex phenomenon, which is described in the main text.

In Fig. 3 we show a comparative plot of $\bar{\mu}_p$ as a function of methanol concentration for various cases. It can be appreciated that by normalizing the data corresponding to $\epsilon_{pc} = 2.0\epsilon$ by a factor two, we can again redeem the universal master curve. Given the solvation volume of a polymer, the energy density is roughly twice when $\epsilon_{pc} = 2.0\epsilon$ compared to $\epsilon_{pc} = 1.0\epsilon$ or it is similar to that of the $\bar{\mu}_p$ for a chain of twice the chain length. Note the master curve can only be obtained by using a chain length N_l dependent function $f(N_l) = 2N_l/(N_l + 1)$, which measures the fractional contribution of the total solvation volume towards a single monomer in a polymer chain. An approximate calculation suggests that the 3/4 contribution of spherically symmetric solvation shell comes from the two end monomers and center monomer's contribution is 1/4. This lead to a contribution of $3/2 + (N_l - 2)/2 = (N_l + 1)/2$, and contribution per monomer will finally lead to a factor $(N_l + 1)/2N_l$, the inversion of which is used as a scaling function $f(N_l)$ to obtain the master curve.

Supplementary Note 4: Kirkwood-Buff Integrals

It is yet important to mention that we have used a rather simple $s - s$, $s - c$ and $c - c$ interactions, where these (co)solvent components interact with the same force-field. This is a good estimate given that the conformational transition is strongly driven by the preferential $p - c$ interaction. To support this claim we have shown Fig. 4, where we present the excess coordination or the Kirkwood-Buff integral (KBI) G_{ij} between various solvent components in a PNIPAm-methanol-water mixture. The data is shown for the all-atom simulations [3] and compared with the experimental data [4]. It can be appreciated that the PNIPAm-methanol excess coordination G_{pm} is much more dominant than the G_{ij} 's between various (con)solvent components. In some cases, we have also varied ϵ_{pc} and also the relative sizes of (co)solvent molecules. Coil-globule-coil scenario is also observed in those cases (data not shown here) [5].

Supplementary References

1. P.-G. de Gennes, *Scaling Concepts in Polymer Physics* (Cornell University Press, London, 1979).
2. Le Guillou, J. C. and Zinn-Justin, J. Critical Exponents for the n-Vector Model in Three Dimensions from Field Theory. *Phys. Rev. Lett.* **39**, 95 (1977).
3. Mukherji, D. and Kremer, K. Coil-Globule-Coil Transition of PNIPAm in Aqueous Methanol: Coupling All-Atom Simulations to Semi-Grand Canonical Coarse-Grained Reservoir. *Macromolecules* **46**, 9158 (2013).
4. Marcus, Y. Preferential Solvation in Mixed Solvents Part 8. Aqueous Methanol from Sub-ambient to Elevated Temperatures. *Phys.Chem.Chem. Phys.* **1** 2975 (1999).
5. Mukherji, D., Marques, C. M. and Kremer, K. Effect of interaction energy and (co)solvent sizes on the conformational transition of polymer in mixed cosolvents: Theory and generic simulation, in preparation (2014).